

Supporting Information

Origin of the increased open circuit voltage in PbS-CdS core-shell quantum dot solar cells

M. J. Speirs,^a D. M. Balazs,^a H.-H. Fang,^a L.-H. Lai,^a L. Protesescu,^{b,c} M. V. Kovalenko,^{b,c} M. A. Loi^a

^a Photophysics & OptoElectronics, Zernike Institute for Advanced Materials, Nijenborgh 4, Groningen, 9747 AG, The Netherlands E-mail: m.a.loi@rug.nl

^b Department of Chemistry and Applied Biosciences, ETH Zürich, Vladimir Prelog Weg 1, Zürich, 8093, Switzerland

^c EMPA-Swiss Federal Laboratories for Materials Science and Technology, Überlandstrasse 129, Dübendorf, 8600, Switzerland, E-mail: mvkovalenko@ethz.ch

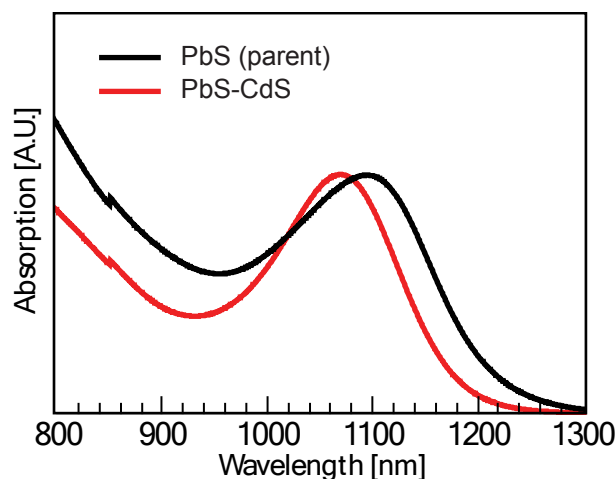


Figure S1. Absorption spectra of the core only QDs used prior to Cd²⁺ cation exchange (black) and the resulting core-shell QDs (red) after cation exchange. A blue shift of ~26 nm can be observed, indicating a reduction of the core size of ~0.1 nm, calculated with the empirical equation of Moreels et al.,¹ relating the bandgap E_g with and the QD size: $E_g = 0.41 + (0.0252d^2 + 0.283d)^{-1}$, where d is the diameter of the QD core.

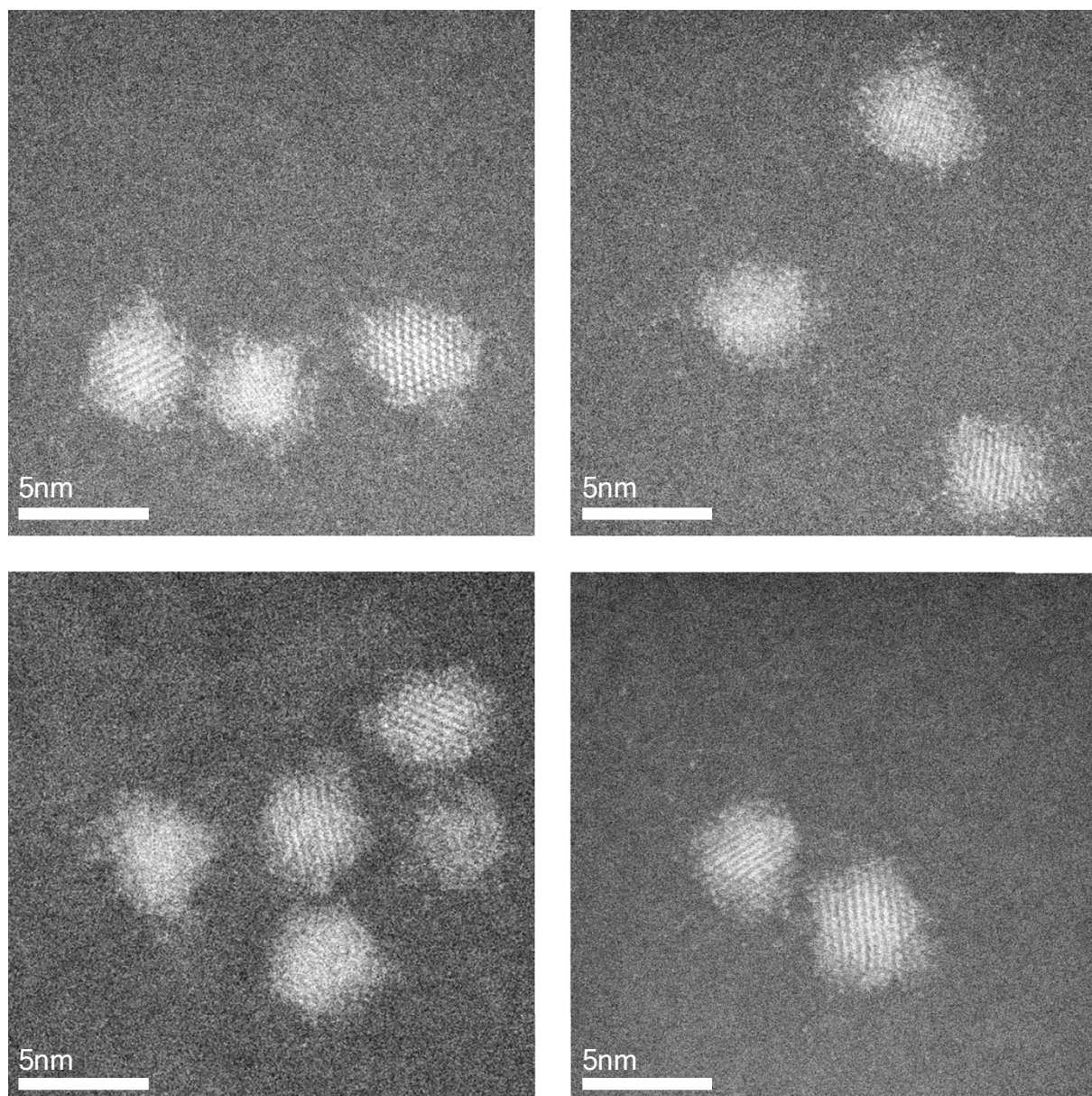


Figure S2. Scanning transmission electron microscope (STEM) micrographs of the core-shell QDs capped with oleic acid. The resolution and the presence of oleic acid ligands prevent clear determination of the shell thickness in these micrographs.

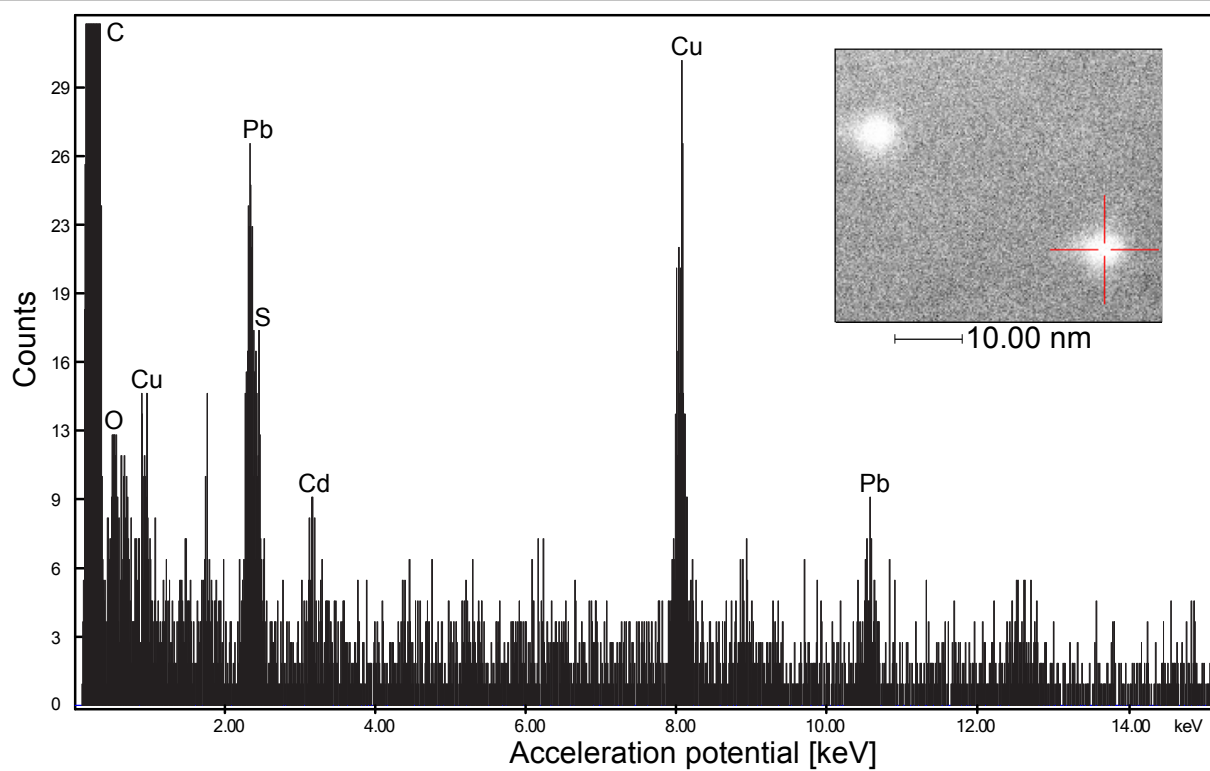


Figure S3. Energy-dispersive X-ray spectroscopy (EDXS) measurement of the core-shell QDs. The atomic labels have been added to the peaks of interest, in particular to indicate the presence of Cd atoms in the shell. The specific QD scanned for this measurement is highlighted in the micrograph in the inset.

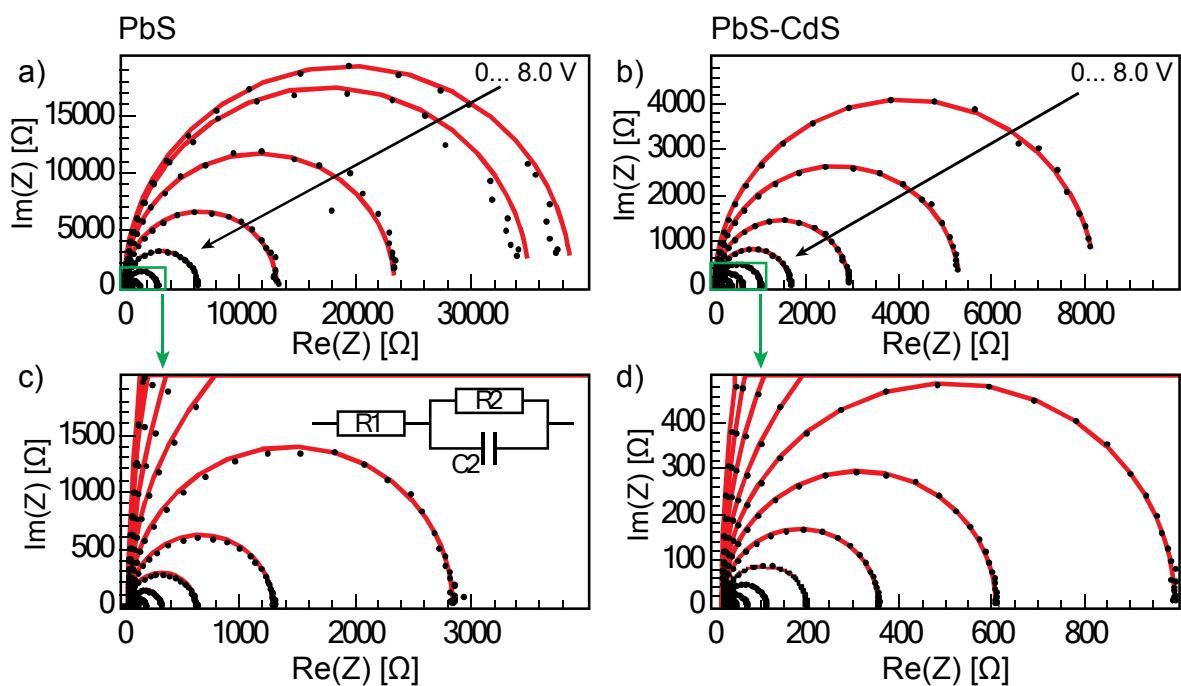


Figure S4. Above: Nyquist plots for a) PbS only and b) PbS-CdS core-shell QDs. Magnifications of the areas highlighted in green are given in c) and d). For these measurements, an oscillating 15 mV bias with frequency ranging from 1 MHz to 10 kHz is applied on top of a constant forward bias, under dark conditions. The constant bias is varied from 0 to 8V in steps of 0.5 V. The measurements (black dots) feature a single arc for both types of QDs. The data are fitted (red lines) using the equivalent circuit displayed in the inset of c). The impedance of this circuit is $Z = R_1 + R_2 / (1 + 2\pi f R_2 C_2)$ and was fitted using the Downhill Simplex algorithm.

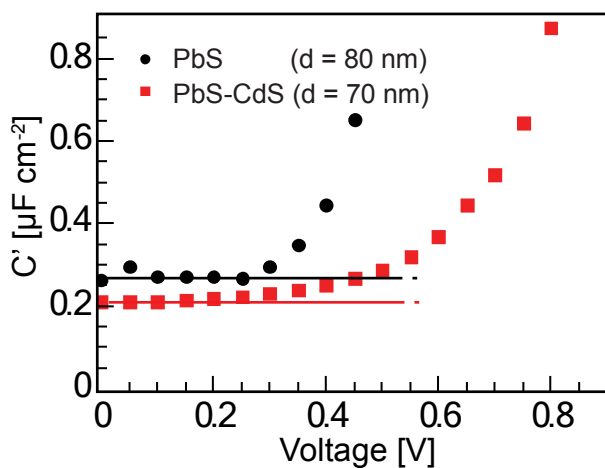


Figure S5. Measurements of capacitance per unit area for core only (black circles) and core-shell QDs (red squares). For this measurement, devices are fabricated with thicknesses (70 – 80 nm) lower than the depletion width (see below) and the capacitance is extracted from the fully depleted region at zero bias. To calculate the relative permittivity ϵ , parallel-plate capacitance $C' = C/A = \epsilon\epsilon_0/d$ is assumed, where A and d are the device area and thickness, respectively, and ϵ_0 is the permittivity of vacuum.

Calculation of the depletion width.

Fully depleted devices are necessary to avoid chemical contributions to the capacitance. The depletion width can

be calculated from $w = \left(\frac{2\epsilon\epsilon_0}{qN}V_{sc}\right)^{1/2}$, where V_{sc} is the voltage over the diode ($V_{sc} = V_{app} - V_{bi} = -V_{bi}$, under zero applied bias), ϵ and ϵ_0 are the relative and vacuum permittivity respectively, and N is the doping concentration.² Doping concentrations of $9.6 \cdot 10^{16} \text{ cm}^{-3}$ and $1.9 \cdot 10^{17}$ were found for the core only and core-shell respectively, as determined from the slope of the Mott-Schottky curves (see Equation 2 and Figure 3). With the permittivities of $\epsilon_{\text{PbS}} = 21\text{-}24$ and $\epsilon_{\text{PbS-CdS}} = 15\text{-}17$ this leads to depletion widths of $124 \pm 5 \text{ nm}$ and $76 \pm 4 \text{ nm}$ for the core only and core-shell QDs, respectively.

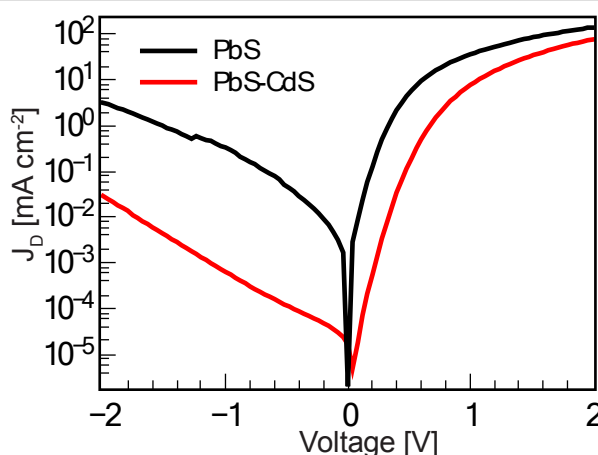


Figure S6 Current-voltage characteristics of the core only (black) and core-shell (red) quantum dot solar cells under dark conditions. Neither curve exhibits a very distinct exponential regime, making the determination of a well-defined ideality factor from these curves difficult.

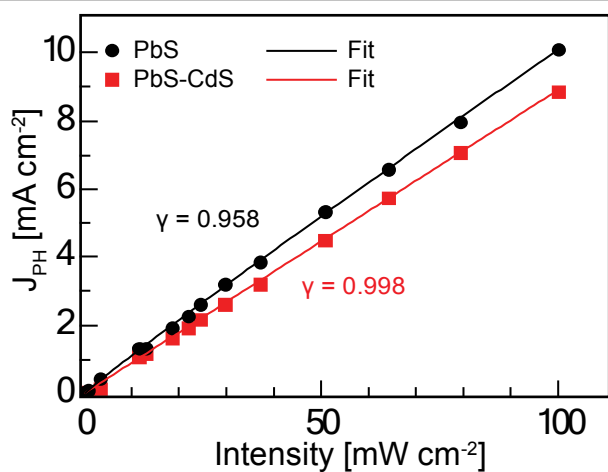


Figure S7. Intensity dependence of the photocurrent at short circuit conditions for the core only QDs (black circles) and core-shell QDs (red squares). The data are fitted with the equation $J(I) = C * I^\gamma$ to determine the degree of linearity of the photocurrent with illumination intensity. The core-shell feature an almost perfect linearity, while the core-only feature a slightly sub-linear illumination dependence.

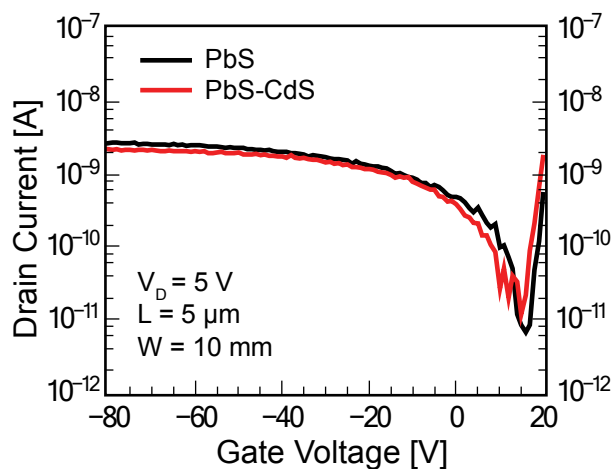


Figure S8. P-channel transfer characteristics for core only QDs (black) and core-shell QDs (red). No significant difference is observed for the hole current, indicating that primarily electron traps are passivated in the core-shell QDs.

1. I. Moreels, K. Lambert, D. Smeets, D. De Muynck, T. Nollet, J. Martins, F. Vanhaecke, A. Vantomme, C. Delerue, G. Allan, and Z. Hens, *ACS Nano*, 2009, **3**, 3023.
2. F. Fabregat-Santiago, G. Garcia-Belmonte, I. Mora-Seró, and J. Bisquert, *Phys. Chem. Chem. Phys.*, 2011, **13**, 9083.